Chemoselective Polymerizations from Mixtures of Epoxide, Lactone, Anhydride, and Carbon Dioxide

JACS
JOURNAL OF THE AMERICAN CHEMICAL SOCIETY
Article
pubs.acs.org/JACS

Chemoselective Polymerizations from Mixtures of Epoxide, Lactone, Anhydride, and Carbon Dioxide

Charles Romain,*[,†] Yunqing Zhu,[†] Paul Dingwall,[†] Shyeni Paul,[†] Henry S. Rzepa,[†] Antoine Buchard,[‡] and Charlotte K. Williams*[,†]

[†]Department of Chemistry, Imperial College London, London SW7 2AZ, U.K.
[‡]Department of Chemistry, University of Bath, Bath BA2 7AY, U.K.

W *Web-Enhanced Feature* *S* *Supporting Information*

ABSTRACT: Controlling polymer composition starting from mixtures of monomers is an important, but rarely achieved, target. Here a single switchable catalyst for both ring-opening polymerization (ROP) of lactones and ring-opening copolymerization (ROCOP) of epoxides, anhydrides, and CO_2 is investigated, using both experimental and theoretical methods. Different combinations of four model monomers—ε-caprolactone, cyclohexene oxide, phthalic anhydride, and carbon dioxide—are investigated using a single dizinc catalyst. The catalyst switches between the distinct polymerization cycles and shows high monomer selectivity, resulting in block sequence control and predictable compositions (esters and carbonates) in the polymer chain. The understanding gained of the orthogonal reactivity of monomers, specifically controlled by the nature of the metal-chain end group, opens the way to engineer polymer block sequences.

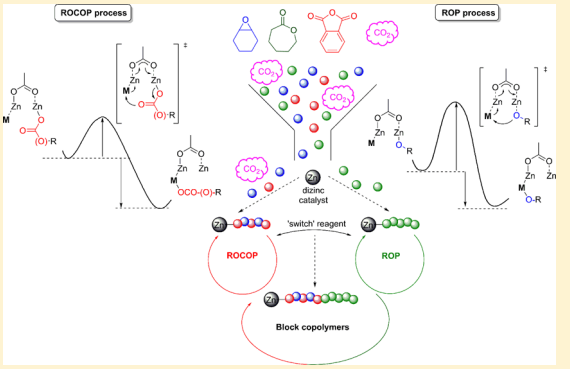

INTRODUCTION

Discovering selective transformations using monomer mixtures to yield polymers of homogeneous compositions, including block sequences, are highly desirable both to reduce costs and to enhance chemical complexity.[1] Block copolymers are important in commodity applications but also allow finer control of properties thereby allowing tailoring for higher-value applications.[2] Pioneering monomer sequence selectivity has been demonstrated in processes including controlled radical polymerizations, stepwise monomer coupling reactions, and ring-opening metathesis polymerization.[1b,3] Nonetheless, significant challenges remain, particularly to expand the methods to oxygenated polymers and to allow controllable enchainment from mixtures. Methods to switch polymerization reactions "on/off" or between different catalytic cycles are generally useful and will be essential to enable block selectivity and diversity.[4] Matyjaszewski and co-workers pioneered an electrochemical "switch", controlling the oxidation state and reactivity of Cu catalysts for atom transfer radical polymerizations.[5] Furthermore, photoelectrochemical triggers can be used to control radical polymerizations.[6] In the distinct area of lactone ring-opening polymerizations (ROP), it is also feasible to switch on/off the reactivity of metal alkoxide catalysts by changing the oxidation state.[7] Using this method it was even possible to discriminate between two very similar monomers, lactide and ε-caprolactone, in ROP.[7c] Mirkin and co-workers demonstrated allosteric switchable polymerization catalysts, whereby the addition of halide ions switched the catalyst conformation enabling a switch on/off ROP.[8] Dubois, Coulembier, and co-workers developed a switch process for ROP of lactone and cyclic carbonates that is controlled by the presence/absence of carbon dioxide.[9]

Kinetic control is of long-standing interest as a means to control polymer composition from mixtures, albeit requiring that a common polymerization method is used. For example, Coates and co-workers discovered that the ring-opening copolymerizations (ROCOP) of an epoxide, anhydride, and carbon dioxide occurred with very high selectivity to yield only block copoly(ester-carbonates).[10] The ROCOP of epoxide/anhydride occurred first, followed by epoxide/CO_2 polymerizations. Subsequently, various other ROCOP catalysts showed the same selectivity allowing various new semi-aromatic polyesters to be prepared.[11,12] Albertsson and co-workers exploited differences in polymerization rates, enhanced using thermal switches, in the ROP of ε-caprolactone and a cyclic carbonate to prepare multi-block copolymers.[13] Stereochemical control is a special case of kinetic selectivity, an outstanding control in lactone ROP was first demonstrated by Coates and Thomas using chiral catalysts and racemic mixtures of two similar, but subtly different, lactones to yield syndiotactic polyesters.[14]

Another strategy in block selectivity is to link together two different polymerization cycles, in the best cases these occur via "one-pot" processes using tandem catalysis and sequential monomer additions.[15] For example, Darensbourg and Lu

Received: December 14, 2015
Published: March 22, 2016

DOI: 10.1021/jacs.5b13070
J. Am. Chem. Soc. 2016, 138, 4120−4131

applied organocatalysts for lactide ROP which were subsequently deactivated by water addition, allowing a second metal catalyst to initiate the ROCOP of epoxide/CO_2.[15b,c,f] Hadjichristidis and Gnanou prepared block copoly(ether-ester/carbonates) using base-catalyzed epoxide ROP, followed by addition of an organo-catalyst to deactivate the base and simultaneously initiate lactone/cyclic carbonate ROP.[16]

In 2014, our group reported the first example of a *single* catalyst, **1** (Supporting Information (SI), Figure S1), which was active for two distinct polymerization cycles and which could be "switched" between them by a new type of chemoselective control. The selectivity arises by controlling the chemistry of the metal−polymer chain end group, with metal alkoxides and carbonates having orthogonal reactivities toward the monomers.[17] Using this method, mixtures of cyclohexene oxide, ε-caprolactone, and carbon dioxide were first polymerized by ROCOP (epoxide/CO_2) to produce a perfectly alternating polycarbonate block and, once the carbon dioxide was consumed/removed, the same catalyst selectively polymerized the lactone, by ROP, ultimately producing block copoly(ester-carbonates). This surprising result was rationalized by kinetic phenomena: i.e., relatively faster rate of carbon dioxide insertion into the zinc alkoxide intermediate, which is common to both catalytic cycles. To our knowledge such chemoselective control is conceptually and practically distinct from the previous switches because it operates via control of the chemistry of the chain end group and it applies just one catalyst (and pot) for two distinct polymerization cycles (Scheme 1). Exploiting the "chemoselective switch" allows

Scheme 1. Three Distinct Polymerization Catalytic Cycles Which Are Feasible from the Zinc Alkoxide Intermediate[a]

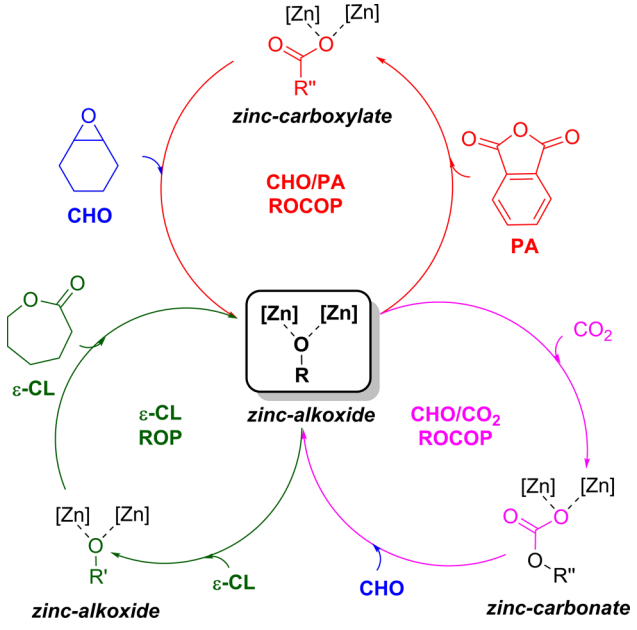

[a]See Figure S1 for dizinc catalyst structure.

epoxides to be used to switch-on catalysts, such as **1**, for efficient ROP of lactones.[18] Furthermore, it can be used to selectively prepare ABA type block copoly(ester-carbonate-esters).[19] Very recently, it was used to prepare multi-block copolyesters, using mixtures of ε-decalactone, phthalic anhydride, and epoxides and switching between ROCOP (epoxide/anhydride) and ROP (lactone).[20] Despite the promising results, the fundamental basis for the selectivity is not yet understood. Here, we combine experimental and theoretical studies to examine the thermodynamic factors under-pinning the selective transformations.

RESULTS AND DISCUSSION

A detailed study comparing the products of polymerizations conducted using mixtures selected from four generic types of oxygenated precursors was undertaken (Scheme 2). The

Scheme 2. Four Exemplar Monomers and the Range of Polymer Products Produced Using Chemoselective Catalysis

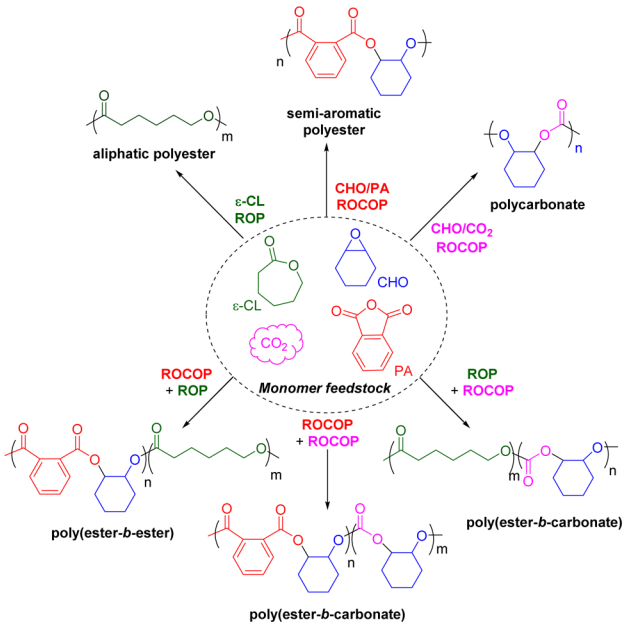

experimental and theoretical products of polymerizations using an epoxide (cyclohexene oxide, CHO), carbon dioxide (CO_2), an anhydride (phthalic anhydride, PA), and a lactone (ε-caprolactone, ε-CL) are compared. In each case, it should be understood that quite a variety of other monomers could be selected, but here the goal is to compare the four exemplar monomers to understand the factors that differentiate particular pathways and thereby provide insight into the observed selectivity. A dizinc catalyst, **1**, is used in every case, its synthesis was previously reported (Figure S1).[17,21] Scheme 2 provides an overview of polymers formed from various monomer combinations. Throughout the study, the catalyst selectivity from all feasible permutations of three monomers was conducted.

Lactone, Epoxide, and CO_2. Polymerizations from mixtures of CO_2, epoxide, and ε-CL were investigated (Figure 1). Initially, it was confirmed that catalyst **1** on its own is not active for the ε-CL ROP under any experimental conditions, including at high temperature (130 °C) and using concen-

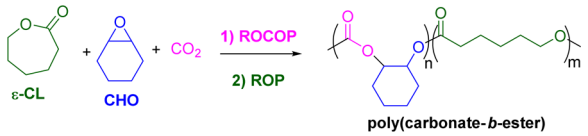

Figure 1. Poly(carbonate-*block*-ester) formation from mixtures of ε-caprolactone (ε-CL), cyclohexene oxide (CHO), and CO_2.

DOI: 10.1021/jacs.5b13070
J. Am. Chem. Soc. 2016, 138, 4120−4131

trations of monomer from 1 to 8 M (Table S1). However, the rapid and quantitative ROP of ε-CL was possible after the addition of epoxide, either as a sub-stoichiometric quantity (~10 equiv vs **1**, in toluene) or as the solvent (Figure 1 and Table 1, runs 1–4). The "switch-on" of ROP occurred due to

Table 1. Polymerizations Using Lactone, Epoxide, and CO_2[a]

run no.	1/CHO/ε-CL (equiv)	CO_2 (atm)	time	conv[b] (%) ε-CL	conv[b] (%) CHO	M_n ($Đ$)[c] (kg·mol^{-1})
1	1/800/200	0	45 min	100	0	7.4 (1.90)
2	1/600/400	0	40 min	100	0	22.2 (1.50))
3	1/400/600	0	35 min	100	0	38.0 (1.4)
4	1/200/800	0	45 min	58	0	44.9 (1.4)
5	1/900/100	1	20 h	0	15	1.0 (1.08)
6	1/100/900	1	17 h	0	0	0
7	1/400/600	1	8.5 h	0	0	0

[a]Reaction conditions: **1** = 1 equiv, 80 °C, monomer mixture as solvent. [b]Conversion determined by ^{1}H NMR spectroscopy (see SI). [c]Determined by SEC, with polystyrene standards.

the reaction of **1** with the epoxide to form an alkoxide intermediate, which was characterized by *in situ* using FTIR spectroscopy (Figure S1).[22] The spectroscopic study confirmed that the acetate co-ligand of catalyst **1** attacks CHO, forming a zinc alkoxide; it is this alkoxide which is an active initiator for ROP (Figure 2).

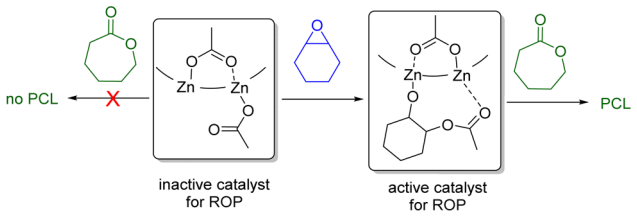

Figure 2. *In situ* catalyst activation for the ring-opening polymerization (ROP) of ε-CL.

The rapid polymerization of ε-CL, catalyzed by **1** in the presence of epoxide, over a range of loadings (**1**:monomer 1:200–800 mol/mol), results in quantitative conversion to poly(caprolactone) (PCL) in less than 1 h (Table 1, runs 1–4). The PCL molecular weight (MW) can be controlled over the range 6–45 kg·mol^{-1} (Table 1 and Figure S2). The catalyst system is highly active, having a turnover frequency of 620 h^{-1} (Table 1, run 4), which compares well with some of the best systems.[23] The polymerization control is high, as assessed by an aliquot method; there is a linear relationship between MW and conversion (Figure 3) and a linear relationship between MW and 1/[**1**] (Figure S2). Importantly, despite there being two strained heterocycles present, both of which could undergo ROP, there is no evidence of incorporation of any epoxide either in the polyester, i.e., no ether linkages, or as a separate polyether. That is, the catalyst is highly selective for lactone ROP.

When catalyst **1** is reacted with a mixture of ε-CL, epoxide, and CO_2, only polycarbonate (PCHC) is formed (Table 1, run 5),[17] and under these conditions there is no lactone incorporation (see Figure S3). Further, polymerizations using mixtures of lactone, epoxide, and CO_2, conducted using high concentrations of ε-CL (Table 1, entries 6 and 7), were unsuccessful and no polycarbonate formed (Figure S4). This

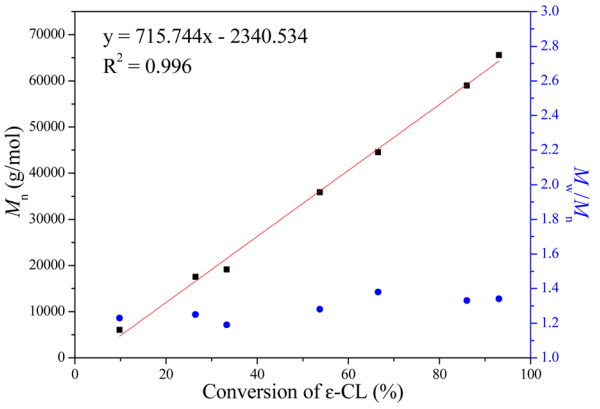

Figure 3. Shows a plot of the PCL M_n (black squares) and M_w/M_n (blue dots) versus ε-CL conversion. Reaction conditions: **1**/CHO/ε-CL = 1/600/2000, 80 °C.

finding was proposed to be caused by competitive coordination of ε-CL at the catalyst preventing copolymerization occurring by blocking epoxide binding. In order to understand the influence of CO_2 on ROP, the polymerization of ε-CL (600 equiv) was conducted, under a nitrogen gas atmosphere in the presence of CHO (2000 equiv), with the gas atmosphere exchanged to CO_2 after 36 min (Figure S5).

Analysis using *in situ* ATR-IR spectroscopy shows that shortly after CO_2 addition there is complete cessation of the polymerization, with the ε-CL conversion remaining at 70% by ^{1}H NMR spectroscopy (Figure S6). The short time (~6 min) taken to completely stop polymerization likely corresponds to the rate of CO_2 dissolution. Indeed, using other related catalysts, if vacuum is applied prior to CO_2 addition, immediate cessation of polymerization occurred.[19] Careful analysis of the polymer, using NMR spectroscopy, showed only PCL formation; there was no evidence for any CO_2 insertion into the polymer backbone (Figure S6). The zinc alkoxide intermediate, generated by reaction between **1** and CHO, immediately formed a new zinc carbonate species on exposure to just 1 bar pressure of CO_2 (as monitored by ATR-IR spectroscopy, Figure S1).[22] Other researchers have also recently reported that CO_2 can be used to inhibit ROP of either ε-CL or cyclic carbonates, using quite different organocatalysts.[9] Thus, there is growing evidence that either metal or organic carbonate species are not viable initiators/catalysts for lactone ROP.

In order to shed light on the high degrees of selectivity observed experimentally, a DFT study was undertaken. It should be noted that the CHO/CO_2 ROCOP process using catalyst **1** has already been studied by DFT;[22] therefore, the same level of theory was applied. For all calculations, the ωB97XD/6-31G(d)/SCRF (cpcm, solvent = dichloromethane) protocol was used. In fact, this protocol yields results in close agreement to those determined using higher basis sets (see Tables S7 and S8) and to those obtained using CCSD calculations; furthermore, the results are in excellent agreement with experimentally determined activation barriers.[22] The calculations were conducted at the same temperatures as applied experimentally (ROP ε-CL, ROCOP CHO/CO_2 = 80 °C, and ROCOP PA/CHO = 100 °C). It is notable that there are very few theoretical studies of epoxide/CO_2,[24] as yet there are none for epoxide/anhydride polymerizations. A recent

DOI: 10.1021/jacs.5b13070
J. Am. Chem. Soc. 2016, 138, 4120–4131

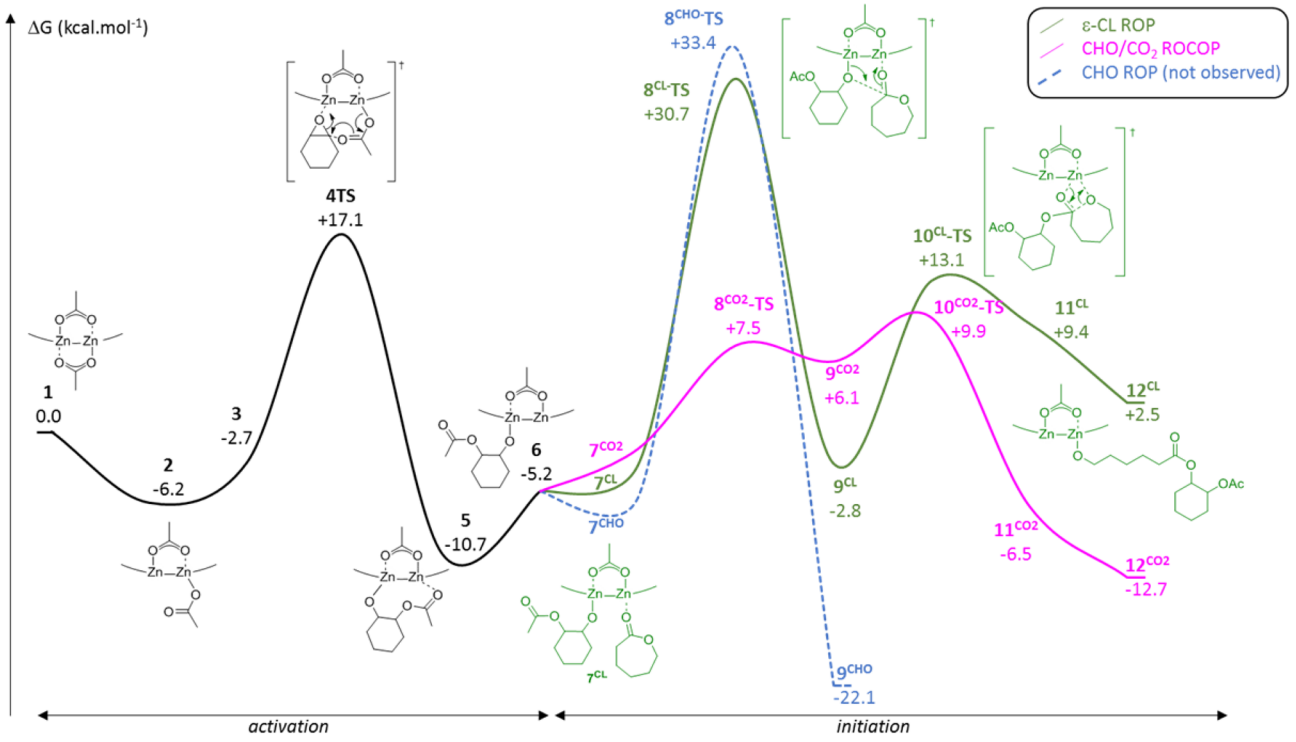

Figure 4. Potential energy surface for activation and initiation in ε-CL ROP (green), CHO/CO_2 ROCOP (purple), or CHO ROP (blue). (Full details are given in Table S3 and Figure S7; data are available at http://doi.org/10.14469/hpc/275.)

review contrasts the theoretical methods applied to this field of catalysis.[25]

The Gibbs free energy profile (including key transition states) was calculated for all possible polymerization reactions between CHO, ε-CL, and CO_2, catalyzed by **1**, and the most viable of these are illustrated in Figures 4 and 5 (all the data are available in the SI, Figures S7 and S8, and Tables S3 and S4). In Figure 4 the reactions corresponding to *Activation* and *Initiation* are shown, whereby the catalyst reacts first with a molecule of epoxide to generate an alkoxide intermediate which subsequently reacts with a molecule of ε-CL. The second monomer addition cycle, illustrated in Figure 5, *Propagation*, whereby the metal alkoxide intermediate reacts with a second molecule of ε-CL. In order to understand the relative barriers to other possible polymerization pathways, the reactions of the alkoxide intermediates (**6** and $\mathbf{12}^{CL}$) with carbon dioxide or epoxide are also illustrated (purple and blue pathways, respectively, Figures 4 and 5).[22]

Considering the *Activation* reaction, it was not possible to locate any transition states or intermediates for the direct attack and ring-opening of ε-CL by catalyst **1**. Experiments show that **1** is not a catalyst, even when significant energy is provided in the form of heating: these results confirm the ring-opening is not thermodynamically favorable. In contrast, **1** can react with CHO (*Activation*) (the energies of various intermediates and transition states are shown in the SI, Table S3 and Figure S7), to form the zinc alkoxide species **6** (ΔG_{353} = −5.2 kcal·mol^{-1}), which was characterized spectroscopically. Importantly, **6** has a coordinative vacancy at one of the zinc centers, resulting from the (growing) polymer chain rotating away from the metals, and is the common intermediate from which the various monomer additions are compared. It is also thermodynamically favorable compared to the isolated starting species (**1** + epoxide), due to the relatively high ring-strain of the epoxide. Intermediate **6** can initiate ε-CL ROP by a coordination/insertion mechanism (for the entire pathway see Figure S7), leading to the formation of intermediate $\mathbf{12}^{CL}$ (Figure 4). Coordination of ε-CL forms intermediate $\mathbf{7}^{CL}$ (ΔG_{353} = −2.9 kcal·mol^{-1}) and is followed by intramolecular attack on the lactone by the zinc alkoxide, leading to the hemi-acetal intermediate $\mathbf{9}^{CL}$ (ΔG_{353} = −2.8 kcal·mol^{-1}). The attack occurs via a relatively high energy transition state $\mathbf{8}^{CL}$**-TS** ($\Delta G^{‡}$ = +30.7 kcal·mol^{-1}), in line with the reaction requiring temperatures above 80 °C to occur at an appreciable rate. Intermediate $\mathbf{9}^{CL}$ is able to react further, by ring-opening of the hemi-acetal, leading to the formation of a new zinc alkoxide intermediate, $\mathbf{11}^{CL}$ (ΔG = +9.4 kcal·mol^{-1}). The ring-opening step occurs through a lower energy transition state $\mathbf{10}^{CL}$**-TS** ($\Delta G^{‡}_{353}$ = +13.1 kcal·mol^{-1}) involving acyl bond cleavage and zinc alkoxide bond formation. A slightly more stable intermediate $\mathbf{12}^{CL}$ (ΔG_{353} = +2.5 kcal·mol^{-1}) has a coordinative vacancy and is proposed as the intermediate for further propagations (Figure 4). Other groups have studied ε-CL ROP, using DFT, and have isolated related transition states and found that the process may be exergonic.[26]

The alternative pathway, which is not observed experimentally, whereby intermediate **6** reacts with a second epoxide molecule, via a coordination/insertion pathway, was also considered (Figure 4, blue pathway). Accordingly, the barrier to epoxide ring-opening is significantly higher ($\Delta\Delta G_{353}$ = +39.1 kcal·mol^{-1} between $\mathbf{7}^{CHO}$ and $\mathbf{8}^{CHO}$**-TS**) compared to that for ε-CL ring-opening ($\Delta\Delta G_{353}$ = +33.6 kcal·mol^{-1} between $\mathbf{7}^{CL}$ and $\mathbf{8}^{CL}$**-TS**). Nonetheless, the putative alkoxide intermediate formed by epoxide ring-opening would be stabilized (ΔG_{353} = −22.1 kcal·mol^{-1}). In addition, the relative energies for the alternative copolymerization reactions, involving CO_2 and CHO, were considered (Figure 4, purple pathway). In line with the experimental findings, if CO_2 is present, the most

DOI: 10.1021/jacs.5b13070
J. Am. Chem. Soc. 2016, 138, 4120−4131

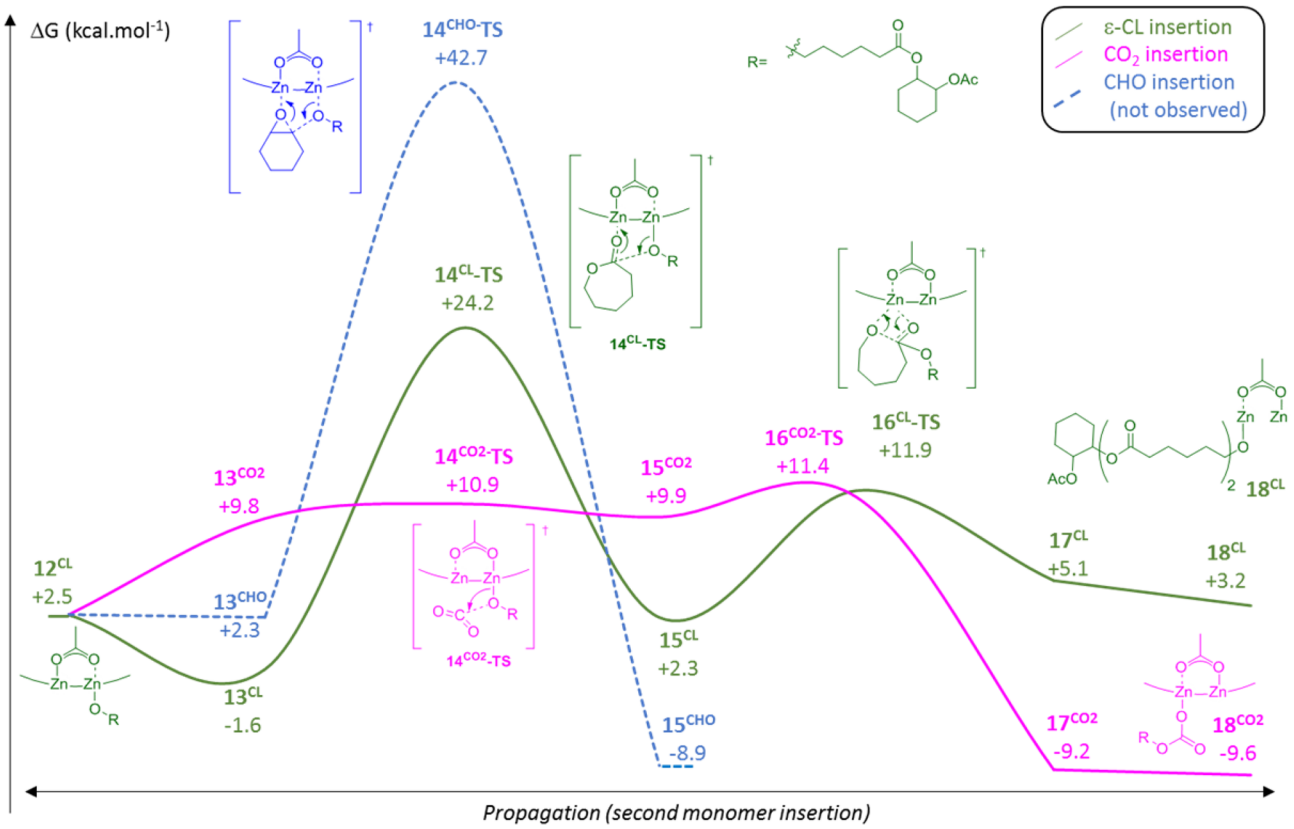

Figure 5. Potential energy surface for ε-CL ROP propagation (green) compared to CHO (blue) or CO_2 insertion (purple). (Full details are given in Table S4 and Figure S8; data are available at http://doi.org/10.14469/hpc/278.)

favorable pathway is via CO_2 insertion, which has a significantly lower energy barrier ($\Delta\Delta G_{353}$ = +11.4 kcal·mol^{-1}) and leads to a stable zinc carbonate intermediate $\mathbf{12}^{CO_2}$ (ΔG_{353} = −12.7 kcal·mol^{-1}). There was no evidence that the zinc carbonate intermediate could subsequently insert an ε-CL molecule. Thus, the theoretical study is in line with the experimental observation that formation of a zinc carbonate prevents ROP.

The propagation pathway for ε-CL ROP leads to identification of various intermediates $\mathbf{12}^{CL}$–$\mathbf{17}^{CL}$ (Figure 5). The overall energies for the propagating species are lower than for the initiation species, and the energy decreases as polymerization progresses. Furthermore, the highest energy barrier, between **13** and $\mathbf{14}^{CL}$-**TS** ($\Delta\Delta G^{\ddagger}$ = +25.8 kcal·mol^{-1}) is significantly lower than the equivalent barrier during initiation ($\Delta\Delta G_{353}$ = +33.6 kcal·mol^{-1}). This is because the barrier to ε-caprolactone ring-opening depends on the nature of the metal alkoxide group: the secondary cyclohexylene alkoxide has a higher barrier than the primary alkoxide group. Such a difference is in line with the experimental observations that the rate of initiation (k_i) (from the secondary alkoxide, cyclohexylene alkoxide) is slower than that of propagation (k_p) (from the primary alkoxide, caproyl alkoxide); the ratio of k_p/k_i was determined to be 8.[18] It was possible to experimentally further exploit the differences in activation barriers: thus, following polymerization of 100 equiv of ε-CL at 80 °C for 2.0 h, subsequent addition of ε-CL (100 equiv), at room temperature, led to formation of PCL (25 °C, 6.0 h), as observed by NMR and SEC analysis (the M_n increases from 8.8 to 18.8 kDa; see Figures S9 and S10, and Table S5).

Other monomer coordination/insertion pathways were also compared. CO_2 inserts via a series of lower energy intermediates/transition states ($\mathbf{13}^{CO_2}$–$\mathbf{16}^{CO_2}$), leading to the formation of a significantly more stabilized zinc carbonate intermediate $\mathbf{18}^{CO_2}$ (ΔG_{353} = −9.6 kcal·mol^{-1}).[22] In addition to lower energy intermediates and transition states, the stabilization may, in part, explain the observed experimental selectivity whereby polymerizations conducted using mixtures of CHO, ε-CL, and CO_2 result only in the formation of polycarbonate. $\mathbf{18}^{CO_2}$ reacts further with CHO, leading to a new zinc alkoxide intermediate $\mathbf{21}^{CO_2}$ (see Figure S8) In contrast, it was not possible to locate a transition state for further reaction of $\mathbf{18}^{CO_2}$ with another lactone. These findings are consistent with the experimental observations that ε-CL remains unreacted during epoxide/CO_2 ROCOP and that addition of CO_2 "easily" switches to the formation of a carbonate intermediate. A further possible side reaction could be the insertion of CHO and thus sequential enchainment of epoxide (by ROP), leading to (poly)ether linkages (Figure 5, blue). However, the transition state for this transformation is likely too high to be accessible ($\Delta G^{\ddagger}_{353}$ = +42.7 kcal·mol^{-1}), which may explain the lack of experimental evidence of such linkages.

Lactone, Anhydride, and Epoxide Polymerizations. Polymerizations from mixtures of anhydride, epoxide, and ε-CL were investigated (Figure 6). **1** can catalyze the ROCOP of phthalic anhydride (PA) and cyclohexene oxide (CHO). The polymerizations occur rapidly, forming perfectly alternating polyesters (>99% ester linkages) with very high selectivity (Table 2, run 1). In addition, it was already reported that **1** is a viable catalyst for ε-CL ROP, in the presence of epoxide.

Thus, polymerizations from mixed feedstock of anhydride, epoxide, and ε-CL was investigated. The mixture polymerization, monitored using *in situ* ATR-IR spectroscopy,

DOI: 10.1021/jacs.5b13070
J. Am. Chem. Soc. 2016, 138, 4120–4131

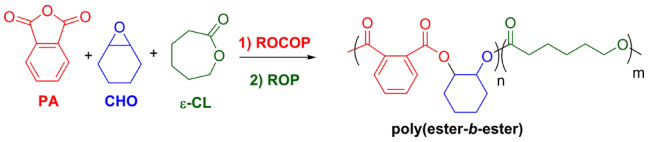

Figure 6. Poly(ester-*block*-ester) formation from mixture of PA, CHO, and ε-CL.

Table 2. Polymerizations of ε-CL, CHO, and PA, Catalyzed by 1[a]

run no.	1/CHO/PA/ε-CL (equiv)	M_n ($Đ$)[b] (kg·mol^{-1})	PCL linkages (%) expt[c]	PCL linkages (%) theor[d]
1	1/800/100/0	2.6 (1.42)	0	0
2	1/400/20/100	12.2 (1.42)	19	17
3	1/400/20/150	15.8 (1.43)	14	12
4	1/400/20/200	18.7 (1.57)	9	9
5	1/400/10/150	22.5 (1.46))	8	6

[a]Reaction conditions: **1** = 1 equiv, 100 °C, monomer mixture as the solvent. All polymerizations were run to complete conversion (>99%) of PA and ε-CL. [b]Determined by SEC, using calibration with polystyrene standards. [c]Determined by ^{1}H NMR spectroscopy, by comparing the relative integrals of the signals assigned to PCHPE ester groups (5.16 ppm) compared with those assigned to PCL ester groups (4.07 ppm) in the copolymers. [d]Calculated using the initial ratio of monomers.

proceeded highly selectively to give block copolyesters. First, the anhydride/epoxide ROCOP occurred (Figure 7), as evidenced by a decrease in resonances assigned to PA and by a concomitant increase in the semi-aromatic polyester absorption (PCHPE). During this phase (almost 2.5 h), there was no change in intensity of the resonances assigned to ε-CL, nor any evidence for PCL formation (by ^{1}H NMR spectroscopy, Figure S11). Only after the anhydride was completely consumed, could ε-CL polymerization occur, rapidly yielding PCHPE−PCL block copolymer, in less than 10 min, as shown by the increase in the resonance at 1240 cm^{-1} assigned to PCL and decrease in the signal at 694 cm^{-1} assigned to ε-CL (for NMR and SEC data see Figures S12 and S13).

A range of different monomer feed ratios were tested (Table 2, runs 2−5), showing close agreement between predicted and experimentally determined compositions and the ability to control the MW. SEC analysis (after isolation of the polymer by precipitation) indicates good control of the MW, indeed the MW increased from 2.6 kg·mol^{-1} (aliquot withdrawn during ROCOP) to 22.5 kg·mol^{-1} for the block copolyester (Figure S13, #5).

SEC analysis, using a UV−vis detector, confirms the presence of aromatic moieties on polymer chains from both aliquots, as required for a block copolymer (Figure S14). The ^{1}H NMR spectra confirm selective block copolyester formation: (i) The resonances assigned to PCHPE end-groups (at 4.65 and 3.46 ppm, see Figure S12) totally disappear after the ROP of ε-CL. (ii) The ratio of PCHPE:PCL signals, as determined by integration, remains constant and in agreement with the monomer feed ratio, regardless of any washing/purification by precipitation of the polymers (Table 2), suggesting that any content of homopolymers (PCHPE or PCL) is not within the detection limits of this spectroscopy (<5%). In addition, a DOSY NMR spectrum of the copolymer shows the same diffusion coefficient for the signals of both PCHPE and PCL blocks, suggesting they are linked (Figure S15).[27] Furthermore,

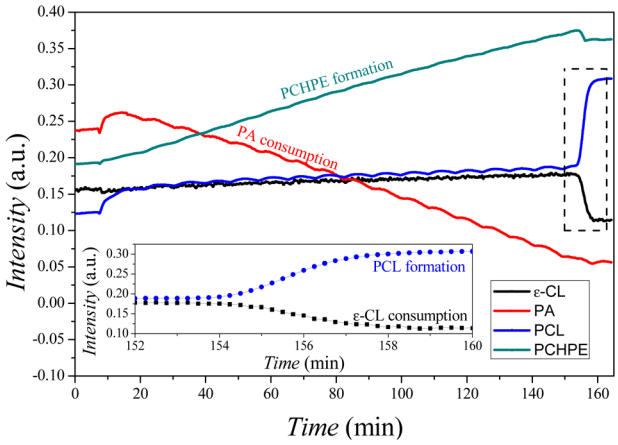

Figure 7. Time-resolved ATR-IR spectra during the polymerization of mixtures of PA, CHO, and ε-CL. The spectra show that ROCOP of PA/CHO occurs first (producing PCHPE), followed by ROP of ε-CL to produce a copolymer (PCHPE−PCL). Inset: enlarged spectra of the time period during which ε-CL ROP occurs. Reaction conditions: 1/CHO/PA/ε-CL = 1/400/20/200, 100 °C, monomer mixture as the solvent.

no extra signals attributed to PCL or PCHPE homopolymers are observed in the DOSY spectrum. For reference, mixing isolated samples of the polymers results in two different signals attributed to the different solution properties (diffusion coefficients) in the blend (Figure S16).

It is notable that PA/CHO copolymerization occurs before ε-CL polymerization even though this latter reaction is significantly faster. The addition of phthalic anhydride during ε-CL ROP quickly stops propagation (Figure S17). The selectivity is attributed to the PA insertion into the Zn−O bond being more favorable compared to ε-CL insertion.

To better understand the thermodynamic influences, DFT calculations were performed under the same conditions (Figure 9). To our knowledge, this is the first such theoretical study of polyester formation by ROCOP. The epoxide/anhydride copolymerization is conducted at slightly higher temperatures (100 °C), so intermediates **1**−**6** were re-optimised (intermediate **1′**−**6′**) at the experimental temperature, leading to only minor changes in energy (Tables S3 and S6). From the common zinc alkoxide intermediate **6′**, coordination of anhydride leads to intermediate $\mathbf{7}^{\mathbf{PA}}$ (ΔG_{373} = −1.6 kcal·mol^{-1}). There are in fact, two enantiomeric approaches during the ring-opening of PA by the CHO alkoxide, and so two transition states for $\mathbf{8}^{\mathbf{PA'}}$**-TS** ($\Delta G^{\ddagger}_{373}$ = +11.7 kcal·mol^{-1}) were found. Both structures and transition states are essentially isoenergetic, with almost identical activation barriers, and as both would lead to the same product after ring-opening, i.e., intermediate **12**, only one pathway was studied further. The "forward" intrinsic reaction coordinate calculation from $\mathbf{8}^{\mathbf{PA'}}$**-TS** (Figures S18 and S19) showed two hidden intermediates, $\mathbf{9}^{\mathbf{PA'}}$ and $\mathbf{10}^{\mathbf{PA'}}$, leading to intermediate $\mathbf{11}^{\mathbf{PA'}}$ (ΔG_{373} = −28.9 kcal·mol^{-1}). These structures involve the ring-opening of the anhydride, followed by cleavage of the cyclohexyl Zn−O bond and coordination of the carboxylate oxygen at the other zinc center. These hidden intermediates are not true stationary points on the potential energy surface, as their first derivatives never quite approach zero, but can be thought of as frustrated minima which can only be characterized in the context of the IRC pathway.[28] Intermediate $\mathbf{11}^{\mathbf{PA'}}$ is thermodynamically favored compared to the previous intermediates (ΔG_{373} =

DOI: 10.1021/jacs.5b13070
J. Am. Chem. Soc. 2016, 138, 4120−4131

−28.9 kcal·mol^{-1}). Intermediate $\mathbf{12}^{\mathbf{PA'}}$ is stabilized (ΔG_{373} = −14.1 kcal·mol^{-1}) and features a coordinative vacancy at the metal center, which is essential for forward polymerizations, for example leading to intermediate $\mathbf{13}^{\mathbf{PA'}}$ (ΔG_{373} = −14.0 kcal·mol^{-1}). The latter undergoes intramolecular nucleophilic attack of the zinc carboxylate at the epoxide and proceeds via a transition state, $\mathbf{14}^{\mathbf{PA'}}$**-TS** ($\Delta G^{\ddagger}_{373}$ = 10.4 kcal·mol^{-1}). The overall energy barrier for CHO insertion ($\mathbf{13}^{\mathbf{PA'}}$, $\mathbf{14}^{\mathbf{PA'}}$**-TS**) is expected to be accessible ($\Delta\Delta G_{373}$ = +24.4 kcal·mol^{-1}) and leads to the formation of intermediate $\mathbf{15}^{\mathbf{PA'}}$ (ΔG_{373} = −11.9 kcal·mol^{-1}), where a new zinc alkoxide bond is formed and a cyclohexylene oxide group has been inserted. Thus, the free energy profile for CHO/PA ROCOP is expected to be driven in part by the thermodynamic stability of some of the ring-opened intermediates.

The energy profile for epoxide/anhydride polymerization is also compared to the ROP of ε-CL (Figure 10). Starting from the common zinc alkoxide intermediate **6″**, there is little energy difference between the coordination of the anhydride and lactone monomers. However, the energy barrier to ring-open the anhydride is significantly lower than that to open the lactone ($\Delta\Delta G^{\ddagger PA''}$ = +15.5 kcal·mol^{-1} vs $\Delta\Delta G^{\ddagger \varepsilon\text{-CL}''}$ = +34.4 kcal·mol^{-1}). Furthermore, when comparing the energy of the intermediate after ring-opening, $\mathbf{11}^{\mathbf{PA''}}$ or $\mathbf{11}^{\mathbf{CL''}}$, it is clear that ROCOP results in a significantly lower energy intermediate ($\Delta G^{PA''}$ = −23.2 kcal·mol^{-1} vs $\Delta G^{\varepsilon\text{-CL}''}$ = +15.2 kcal·mol^{-1}), signaling a thermodynamic driving force favoring ROCOP.

Epoxide, Anhydride, and Carbon Dioxide Polymerizations. Mixtures of CHO, PA, and CO_2 were polymerized selectively by catalyst **1** using ROCOP, to form only copoly(ester-*block*-carbonates).[12c] First, epoxide/anhydride copolymerization occurred, until complete consumption of PA, after which point epoxide/CO_2 copolymerization occurred (Figures 8 and S20).

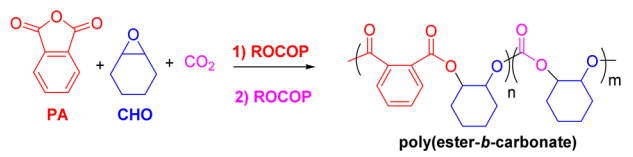

Figure 8. Poly(ester-*block*-carbonate) formation from mixture of PA, CHO, and CO_2.

Once again, the calculated energy profiles at 100 °C for both polymerizations were compared (Figure 11). From the common zinc alkoxide intermediate **6′**, either PA or CO_2 is coordinated, leading to intermediates $\mathbf{7}^{\mathbf{PA'}}$ and $\mathbf{7}^{\mathbf{CO_2}}$, respectively, which are of very similar energy. Next, insertion into the zinc alkoxide bond occurs (via transition states $\mathbf{8}^{\mathbf{PA'}}$**-TS** and $\mathbf{8}^{\mathbf{CO_2'}}$**-TS**, whose energies are less than 5 kcal·mol^{-1} different). As stated, experimentally PA insertion occurs before CO_2 insertion, furthermore CO_2 is not polymerized at all in the presence of PA. This could be attributed, in part, to the lower energy of intermediate $\mathbf{11}^{\mathbf{PA'}}$, compared to $\mathbf{11}^{\mathbf{CO_2'}}$. This energetic stabilization may be sufficient that CHO/PA ROCOP is essentially irreversible and therefore the dominant pathway of the two competing options.

Comparison of Monomer Selectivity. The dizinc catalyst shows unexpected chemoselectivity in polymerizations using different monomer mixtures yielding predictable compositions and block sequences in copolymers. The monomers are polymerized using two distinct catalytic cycles: the ring-opening copolymerizations (ROCOP) of epoxides/CO_2 or epoxides/anhydrides and the ring-opening polymerizations (ROP) of lactones. It is feasible for one catalyst to bridge the two distinct cycles as both involve a zinc alkoxide intermediate (Scheme 1). Experimentally the preference for addition into the zinc−alkoxide bond follows the trend PA > CO_2 > ε-CL, and by exploiting this finding copoly(ester-carbonates) and copoly(esters) are formed (Scheme 2).

In order to understand and compare the elementary steps in the polymerization cycles, a series of DFT studies were undertaken considering two cycles of monomer additions and different permutations of the monomers. Common to all the polymerizations was the zinc alkoxide intermediate **6**, generated by the reaction between the catalyst, zinc acetate, and an epoxide molecule. Figure 12 and Table 3 summarize the limiting energy barriers to the key transition states ($\Delta_{TS}\Delta G$) and the free energy differences ($\Delta_{Pd}\Delta G$) between the corresponding intermediates in the various polymerization cycles.

Epoxide/Anhydride/CO_2. Of the combinations of monomers investigated, only mixtures of epoxides/anhydrides/CO_2 have been explored previously. In those studies, it was observed that various different types of homogeneous catalysts gave rise to high degrees of selectivity. Generally, the anhydride/epoxide ROCOP occurred prior to the CO_2/epoxide reaction.[10,11a−c,12a,c,d,29] In the field of heterogeneous catalysis, there was much less discrimination between the monomers, with studies using zinc glutarate or zinc−cobalt double metal cyanides resulting in the formation of tapered or gradient block copoly(ester-carbonates).[30] The rationale for the observed selectivity was always kinetic; i.e., it was argued that the rates of insertion of anhydride vs CO_2 into metal alkoxide intermediates determined the order of monomer enchainment. Here, it has been demonstrated that in addition to a kinetic rationale, there are also thermodynamic driving forces which could rationalize the experimental data. In particular, the ester linkage formed after anhydride insertion is significantly more thermodynamically stable compared to the carbonate linkage formed after CO_2 insertion. Furthermore, the calculated barriers for the insertions of either PA or CO_2 are not significantly different, particularly at the relevant temperatures for such reactions, to one another. These findings suggest that the observed selectivity in the terpolymerizations may result from a thermodynamic driving force toward formation of a more stable linkage.[10]

Lactone ROP and Epoxide/Anhydride or Epoxide/CO_2 ROCOP. Mixtures of epoxides, lactones, and carbon dioxide result in selective formation of block copoly(ester-carbonates), whereby the CHO/CO_2 ROCOP occurs prior to the ε-CL ROP.[17] The theoretical study shows a significantly higher barrier to ε-CL insertion, compared to CO_2, starting from the same zinc alkoxide intermediate. Furthermore, the product ester linkage is less stable compared to the carbonate linkage. Thus, in addition to kinetic phenomena governing the polymerization selectivity, the thermodynamic stability of the different linkages may also influence the observed selectivity. It is also notable that the initiation of the first ε-CL unit has a significantly higher barrier compared to subsequent propagation; this is because the initiation reaction involves attack by a secondary alkoxide compared to propagation occurring with attack by a primary alkoxide.

Polymerizations conducted using mixtures of epoxide/anhydride/lactone result in the selective formation of block

DOI: 10.1021/jacs.5b13070
J. Am. Chem. Soc. 2016, 138, 4120−4131

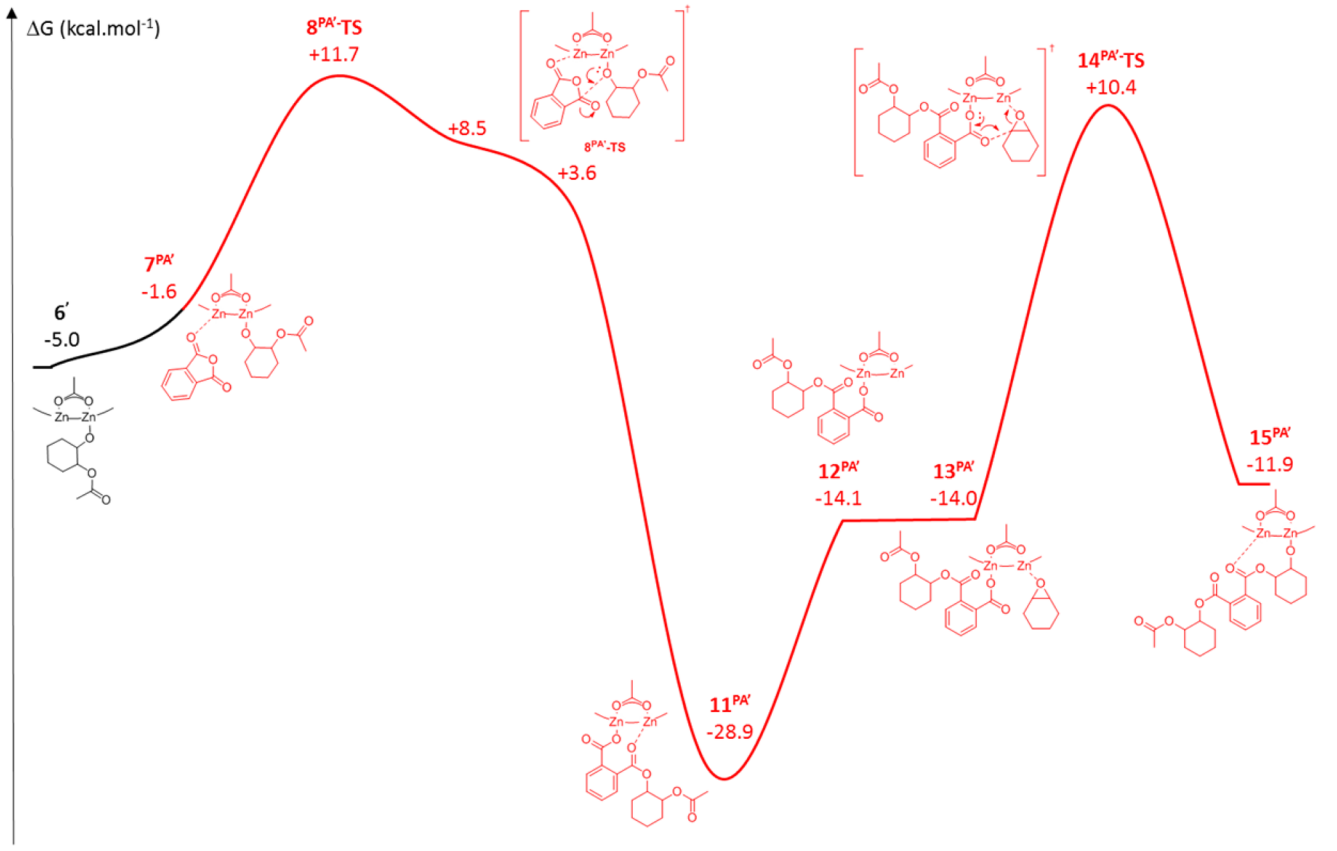

Figure 9. Calculated potential energy surface for ROCOP of CHO/PA that includes two hidden intermediates between $\mathbf{8}^{\mathbf{PA'}}$**-TS** and $\mathbf{11}^{\mathbf{PA'}}$. (Data are available at http://doi.org/10.14469/hpc/281.)

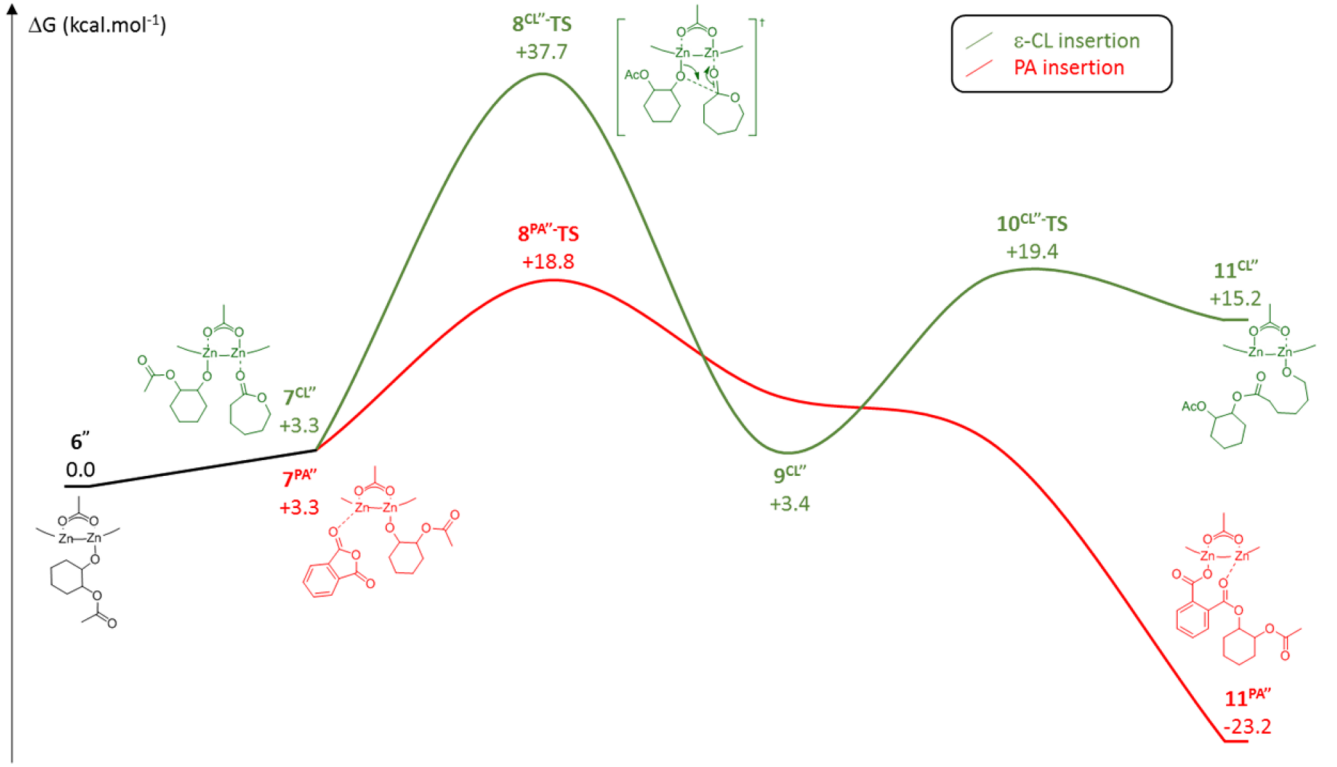

Figure 10. Polymerization pathways from mixtures of CHO, PA, and ε-CL. In red, the ROCOP of CHO/PA; in green, the ROP of ε-CL. (An interactive version of this figure is accessible online.)

DOI: 10.1021/jacs.5b13070
J. Am. Chem. Soc. 2016, 138, 4120−4131

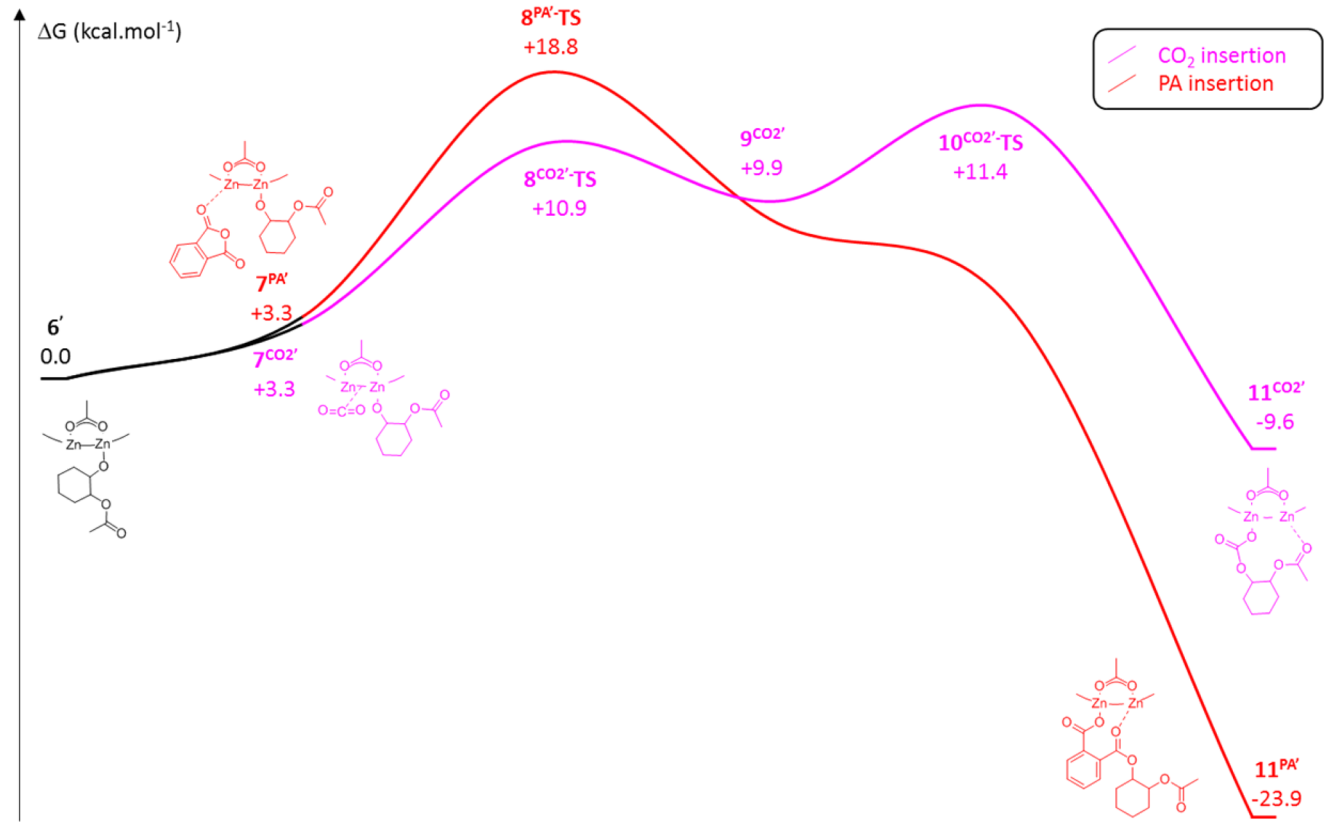

Figure 11. Polymerization pathways for mixtures of CHO, PA, and CO_2. In purple, the ROCOP of CHO/CO_2; in red, the ROCOP of CHO/PA, including two "hidden" intermediates between **8$^{PA'}$-TS** and **11$^{PA'}$** (see Table S6). (An interactive version of this figure is accessible online.)

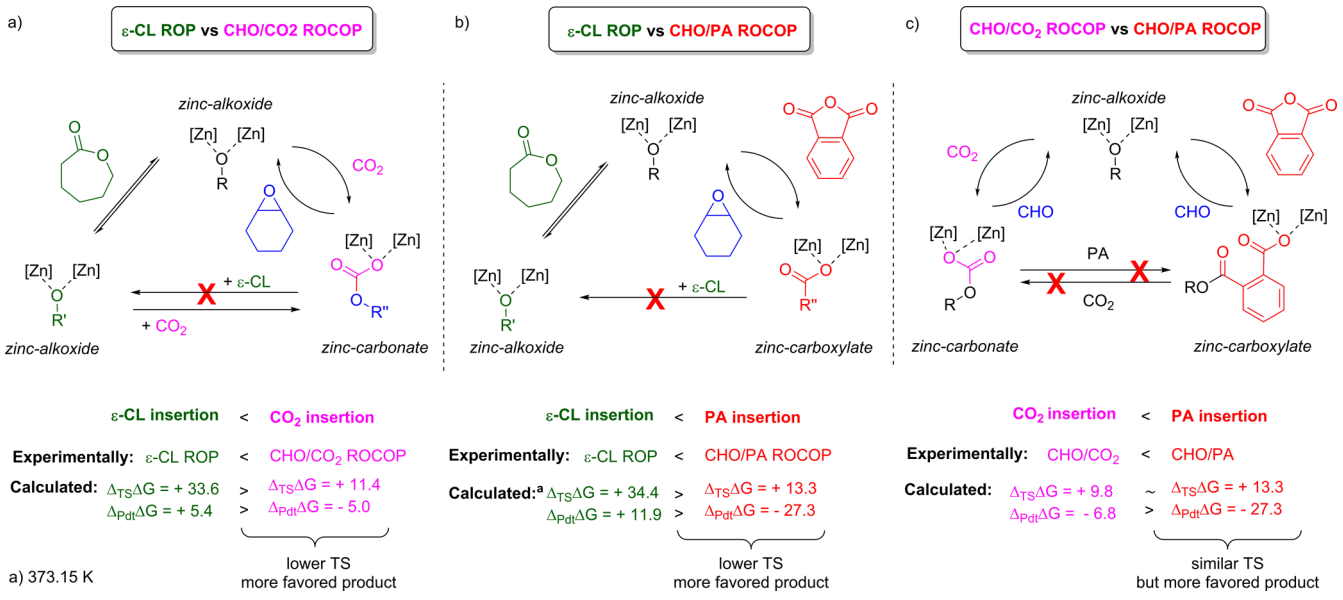

Figure 12. Three polymerization processes, using various permutations of the monomers, compared by experimental and theoretical methods.

copolyesters. The polymerizations progress by the ROCOP pathway until the anhydride is completely consumed, after which time the ROP pathway is accessible. The theoretical study reveals that there is a lower barrier to anhydride insertion, compared to ε-CL ROP, and a greater stability to the product ester linkage formed, thereby also providing a thermodynamic rationale for the observed selectivity.

The study also highlights the importance of considering both a kinetic and thermodynamic basis for future selective polymerizations. Nevertheless, it is also important to consider some other influences over catalytic selectivity. A notable observation is that the catalyst does not enchain epoxide units, and therefore ether linkages are barely detected. It could be concluded from this that sequential epoxide enchainment, by ROP, is not an experimentally accessible pathway, at least at

DOI: 10.1021/jacs.5b13070
J. Am. Chem. Soc. 2016, 138, 4120−4131

Table 3. Illustration and Quantification of the Key Energy Barriers in the Polymerization Processes (kcal·mol^{-1})

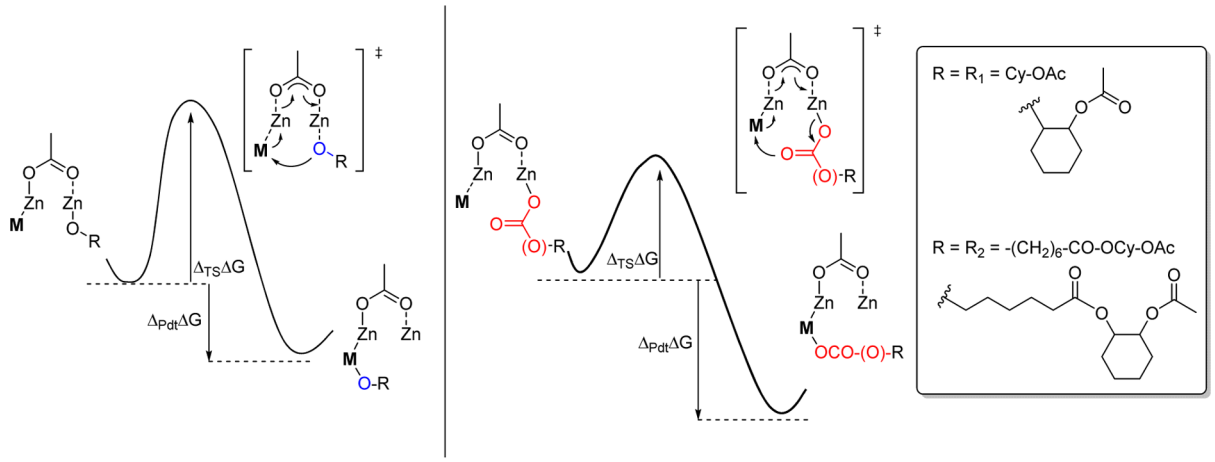

Monomers (M) \ Zn-O bond	Zn alkoxide	Zn carbonate	Zn carboxylate
	R = R$_1$ $\Delta_{TS}\Delta G$ = + 39.1 $\Delta_{Pdt}\Delta G$ = - 16.4 R = R$_2$ $\Delta_{TS}\Delta G$ = + 40.4 $\Delta_{Pdt}\Delta G$ = - 11.2	R = R$_1$ $\Delta_{TS}\Delta G$ = + 23.5 $\Delta_{Pdt}\Delta G$ = + 0.6 R = R$_2$ $\Delta_{TS}\Delta G$ = + 25.3 $\Delta_{Pdt}\Delta G$ = + 0.8	R= R$_1$ $\Delta_{TS}\Delta G$ = + 24.4[a] $\Delta_{Pdt}\Delta G$ = + 2.1[a]
CO_2	R = R$_1$ $\Delta_{TS}\Delta G$ = + 11.4 (+ 9.8)[a] $\Delta_{Pdt}\Delta G$ = - 5.0 (- 6.8)[a] R= R$_2$ $\Delta_{TS}\Delta G$ = + 1.6 $\Delta_{Pdt}\Delta G$ = - 19.0	R = R$_1$ $\Delta_{TS}\Delta G$ = + 10.5[b] $\Delta_{Pdt}\Delta G$ = + 8.2[b]	not observed
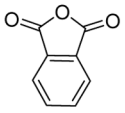	R = R$_1$ $\Delta_{TS}\Delta G$ = + 13.3[a] $\Delta_{Pdt}\Delta G$ = - 27.3[a]	not observed	not observed
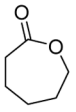	R = R$_1$ $\Delta_{TS}\Delta G$ = + 33.6 (34.4)[a] $\Delta_{Pdt}\Delta G$ = + 5.4 (+11.9)[a] R = R$_2$ $\Delta_{TS}\Delta G$ = + 25.8 $\Delta_{Pdt}\Delta G$ = + 4.8	not observed	not observed

[a]T = 373.15 K. [b]T = 273.15 K.[22]

temperatures up to 100 °C. However, an examination only of the thermodynamic parameters, particularly during initiation, reveals that although the barriers to epoxide insertion are higher than for other monomers, there is a significant stability associated with the putative products. In contrast, during propagation, there is a much more significant differences in the energy barriers, with the epoxide enchainment requiring >10 kcal·mol^{-1} more than the lactone enchainment.

Furthermore, the calculations do not provide kinetic models for initiation/propagation. It is difficult to directly measure the rates of monomer insertion into the zinc−alkoxide bond, particularly in the case of CO_2/anhydride as these are pre-rate-limiting reactions. A recent study of CO_2 insertion into a zinc hydride complex, featuring similar amine−phenolate ligands, revealed that the measured rate in fact corresponded with the rates of CO_2 dissolution/diffusion into the reaction medium (i.e., the reaction was diffusion limited).[31] Given that the rate observed in that study was typical of other zinc complexes reported for CO_2 insertion processes,[32] it seems likely that related insertion reactions may also occur under diffusion-limited conditions. Another factor which would be expected to influence the order of monomer insertion is the concentration of the particular monomer coordinated intermediate. The coordination of the relevant monomer to the catalyst is likely an equilibrium process which would be affected by the relative concentrations of monomers. In the current study, a range of

DOI: 10.1021/jacs.5b13070
J. Am. Chem. Soc. 2016, 138, 4120−4131

different loadings have been explored, and, in most cases, the concentration of the epoxide was significantly greater than that of any other species present. This might be expected to bias somewhat the concentration of the epoxide-coordinated intermediate and thereby enable epoxide enchainment; however, this was never observed experimentally. Finally, it might be expected that if polymerizations could be run at significantly higher temperatures the apparent barrier to epoxide enchainment could be overcome. This is not practical experimentally due to competing factors: (1) ROCOP is an equilibrium processes, where in the case of CO_2/epoxide ROCOP the polymer is the kinetic product, and thus elevated temperatures lead to back-biting and formation of the cyclic carbonate. (2) ROP is also an equilibrium process, and elevated temperatures lead to the back-reaction and increase monomer concentration/polymer degradation. Thus, the epoxide enchainment reaction does not occur using the dizinc catalysts under any of the experimentally studied conditions. This may relate to relatively higher barriers, particularly during propagation, but is not immediately disfavored by the theoretical study. It is interesting to note that various other homogeneous metal complexes have been reported to enchain epoxide units as well as carbonates/esters; thus, there appear to be different influences of the relative barriers/rates which depend on the metal catalysts selected.[12a,b,33]

CONCLUSIONS

Selecting monomers from a mixture so as to construct complex (multi-block) copolymers is a long-standing challenge in polymer chemistry. Usually, copolymer composition is predicted on the basis of empirical monomer reactivity ratios. In this study, a new catalytic approach where a single catalyst can switch between different polymerization cycles and mechanisms enables the selective preparation of copolymers from mixtures of four different monomers. The catalysis is explored using both experimental and DFT studies of all possible monomer combinations using ε-caprolactone, phthalic anhydride, carbon dioxide, and cyclohexene oxide. Block copolyesters and copoly(ester-carbonates) are selectively formed experimentally, and the DFT study reveals that the selectivity results both from lower activation barriers and from more stable intermediates (linkages) in the polymerization pathways. The findings are important as previous attempts to rationalize selective behavior have only considered kinetic phenomena. Given the applications and fundamental interest in block copolymers and degradable, oxygenated polyesters/carbonates, this study has broader implications. In particular, the investigation of other catalysts and other monomer combinations is certainly warranted, and with the detailed understanding of the factors controlling the selectivity in hand it is appropriate to apply this knowledge to prepare more complex and sophisticated polymer architectures.

ASSOCIATED CONTENT

Supporting Information

The Supporting Information is available free of charge on the ACS Publications website at DOI: 10.1021/jacs.5b13070. Complementary data are available from the Imperial College High Performance Computing Service Data Repository at http://doi.org/10.14469/hpc/244.

Experimental procedures and spectroscopic characterization, including Figures S1−S33 and Tables S1−S8 (PDF)

Web-Enhanced Features

Interactive versions of Figures 10 and 11 are accessible in the HTML version of the article.

AUTHOR INFORMATION

Corresponding Authors

*c.romain@imperial.ac.uk

*c.k.williams@imperial.ac.uk

Notes

The authors declare the following competing financial interest(s): C.K.W. is a director at Econic Technologies.

ACKNOWLEDGMENTS

The EPSRC (EP/K035274/1, EP/L017393/1, EP/K014070/1, EP/K014668/1), Roger and Sue Whorrod (fellowship to A.B.), and the CSC (studentship to Y.Z.) are acknowledged for research funding. We thank Imperial College London HPC and EPSRC NSCCS (CHEM826) for computing resources.

REFERENCES

(1) (a) Colquhoun, H.; Lutz, J. F. *Nat. Chem.* **2014**, *6*, 455−456. (b) Lutz, J.-F.; Ouchi, M.; Liu, D. R.; Sawamoto, M. *Science* **2013**, *341*, 628. (c) Mutlu, H.; Lutz, J. F. *Angew. Chem., Int. Ed.* **2014**, *53*, 13010−13019.

(2) Bates, F. S.; Hillmyer, M. A.; Lodge, T. P.; Bates, C. M.; Delaney, K. T.; Fredrickson, G. H. *Science* **2012**, *336*, 434−440.

(3) (a) Al Ouahabi, A.; Charles, L.; Lutz, J.-F. *J. Am. Chem. Soc.* **2015**, *137*, 5629−5635. (b) Li, J.; Stayshich, R. M.; Meyer, T. Y. *J. Am. Chem. Soc.* **2011**, *133*, 6910−6913. (c) Weiss, R. M.; Short, A. L.; Meyer, T. Y. *ACS Macro Lett.* **2015**, *4*, 1039−1043. (d) Gutekunst, W. R.; Hawker, C. J. *J. Am. Chem. Soc.* **2015**, *137*, 8038−8041.

(4) (a) Leibfarth, F. A.; Mattson, K. M.; Fors, B. P.; Collins, H. A.; Hawker, C. J. *Angew. Chem., Int. Ed.* **2013**, *52*, 199−210. (b) Guillaume, S. M.; Kirillov, E.; Sarazin, Y.; Carpentier, J.-F. *Chem. - Eur. J.* **2015**, *21*, 7988−8003.

(5) Magenau, A. J. D.; Strandwitz, N. C.; Gennaro, A.; Matyjaszewski, K. *Science* **2011**, *332*, 81−84.

(6) Fors, B. P.; Hawker, C. J. *Angew. Chem., Int. Ed.* **2012**, *51*, 8850−8853.

(7) (a) Gregson, C. K. A.; Gibson, V. C.; Long, N. J.; Marshall, E. L.; Oxford, P. J.; White, A. J. P. *J. Am. Chem. Soc.* **2006**, *128*, 7410−7411. (b) Broderick, E. M.; Guo, N.; Wu, T.; Vogel, C. S.; Xu, C.; Sutter, J.; Miller, J. T.; Meyer, K.; Cantat, T.; Diaconescu, P. L. *Chem. Commun.* **2011**, *47*, 9897−9899. (c) Wang, X.; Thevenon, A.; Brosmer, J. L.; Yu, I.; Khan, S. I.; Mehrkhodavandi, P.; Diaconescu, P. L. *J. Am. Chem. Soc.* **2014**, *136*, 11264−11267. (d) Biernesser, A. B.; Li, B.; Byers, J. A. *J. Am. Chem. Soc.* **2013**, *135*, 16553−16560.

(8) Yoon, H. J.; Kuwabara, J.; Kim, J.-H.; Mirkin, C. A. *Science* **2010**, *330*, 66−69.

(9) Coulembier, O.; Moins, S.; Todd, R.; Dubois, P. *Macromolecules* **2014**, *47*, 486−491.

(10) Jeske, R. C.; Rowley, J. M.; Coates, G. W. *Angew. Chem., Int. Ed.* **2008**, *47*, 6041−6044.

(11) (a) Huijser, S.; Hosseini Nejad, E.; Sablong, R. l.; de Jong, C.; Koning, C. E.; Duchateau, R. *Macromolecules* **2011**, *44*, 1132−1139. (b) Koning, C. E.; Sablong, R. J.; Nejad, E. H.; Duchateau, R.; Buijsen, P. *Prog. Org. Coat.* **2013**, *76*, 1704−1711. (c) Darensbourg, D. J.; Poland, R. R.; Escobedo, C. *Macromolecules* **2012**, *45*, 2242−2248. (d) Hosseini Nejad, E.; Paoniasari, A.; Koning, C. E.; Duchateau, R. *Polym. Chem.* **2012**, *3*, 1308.

(12) (a) Bernard, A.; Chatterjee, C.; Chisholm, M. H. *Polymer* **2013**, *54*, 2639−2646. (b) Harrold, N. D.; Li, Y.; Chisholm, M. H. *Macromolecules* **2013**, *46*, 692−698. (c) Saini, P. K.; Romain, C.; Zhu,

Y.; Williams, C. K. *Polym. Chem.* **2014**, *5*, 6068−6075. (d) Winkler, M.; Romain, C.; Meier, M. A. R.; Williams, C. K. *Green Chem.* **2015**, *17*, 300−306.
(13) Olsen, P.; Odelius, K.; Keul, H.; Albertsson, A.-C. *Macromolecules* **2015**, *48*, 1703−1710.
(14) (a) Kramer, J. W.; Treitler, D. S.; Dunn, E. W.; Castro, P. M.; Roisnel, T.; Thomas, C. M.; Coates, G. W. *J. Am. Chem. Soc.* **2009**, *131*, 16042−16044. (b) Jaffredo, C. G.; Chapurina, Y.; Guillaume, S. M.; Carpentier, J.-F. *Angew. Chem., Int. Ed.* **2014**, *53*, 2687−2691.
(15) (a) Zhou, J.; Wang, W.; Villarroya, S.; Thurecht, K. J.; Howdle, S. M. *Chem. Commun.* **2008**, 5806−5808. (b) Wu, G.-P.; Darensbourg, D. J.; Lu, X.-B. *J. Am. Chem. Soc.* **2012**, *134*, 17739−17745. (c) Darensbourg, D. J.; Wu, G.-P. *Angew. Chem., Int. Ed.* **2013**, *52*, 10602−10606. (d) Kember, M. R.; Copley, J.; Buchard, A.; Williams, C. K. *Polym. Chem.* **2012**, *3*, 1196−1201. (e) Diallo, A. K.; Guerin, W.; Slawinski, M.; Brusson, J. M.; Carpentier, J. F.; Guillaume, S. M. *Macromolecules* **2015**, *48*, 3247−3256. (f) Tang, L.; Luo, W. H.; Xiao, M.; Wang, S. J.; Meng, Y. Z. *J. Polym. Sci., Part A: Polym. Chem.* **2015**, *53*, 1734−1741. (g) Guillaume, S. M.; Kirillov, E.; Sarazin, Y.; Carpentier, J.-F. *Chem. - Eur. J.* **2015**, *21*, 7988−8003.
(16) (a) Zhao, J.; Hadjichristidis, N. *Polym. Chem.* **2015**, *6*, 2659−2668. (b) Zhao, J.; Pahovnik, D.; Gnanou, Y.; Hadjichristidis, N. *Macromolecules* **2014**, *47*, 3814−3822. (c) Zhao, J.; Pahovnik, D.; Gnanou, Y.; Hadjichristidis, N. *J. Polym. Sci., Part A: Polym. Chem.* **2015**, *53*, 304−312.
(17) Romain, C.; Williams, C. K. *Angew. Chem., Int. Ed.* **2014**, *53*, 1607−1610.
(18) Zhu, Y.; Romain, C.; Poirier, V.; Williams, C. K. *Macromolecules* **2015**, *48*, 2407−2416.
(19) Paul, S.; Romain, C.; Shaw, J.; Williams, C. K. *Macromolecules* **2015**, *48*, 6047−6056.
(20) Zhu, Y.; Romain, C.; Williams, C. K. *J. Am. Chem. Soc.* **2015**, *137*, 12179−12182.
(21) (a) Jutz, F.; Buchard, A.; Kember, M. R.; Fredriksen, S. B.; Williams, C. K. *J. Am. Chem. Soc.* **2011**, *133*, 17395−17405. (b) Kember, M. R.; Knight, P. D.; Reung, P. T. R.; Williams, C. K. *Angew. Chem., Int. Ed.* **2009**, *48*, 931−933.
(22) Buchard, A.; Jutz, F.; Kember, M. R.; White, A. J. P.; Rzepa, H. S.; Williams, C. K. *Macromolecules* **2012**, *45*, 6781−6795.
(23) (a) Labet, M.; Thielemans, W. *Chem. Soc. Rev.* **2009**, *38*, 3484−3504. (b) Arbaoui, A.; Redshaw, C. *Polym. Chem.* **2010**, *1*, 801−826.
(24) Ohkawara, T.; Suzuki, K.; Nakano, K.; Mori, S.; Nozaki, K. *J. Am. Chem. Soc.* **2014**, *136*, 10728−10735.
(25) Darensbourg, D. J.; Yeung, A. D. *Polym. Chem.* **2014**, *5*, 3949−3962.
(26) (a) Rosal, I. D.; Poteau, R.; Maron, L. *Dalton Trans.* **2011**, *40*, 11211−11227. (b) Miranda, M. O.; DePorre, Y.; Vazquez-Lima, H.; Johnson, M. A.; Marell, D. J.; Cramer, C. J.; Tolman, W. B. *Inorg. Chem.* **2013**, *52*, 13692−13701. (c) del Rosal, I.; Brignou, P.; Guillaume, S. M.; Carpentier, J.-F.; Maron, L. *Polym. Chem.* **2015**, *6*, 3336−3352. (d) Barros, N.; Mountford, P.; Guillaume, S. M.; Maron, L. *Chem. - Eur. J.* **2008**, *14*, 5507−5518.
(27) (a) Bakkour, Y.; Darcos, V.; Li, S.; Coudane, J. *Polym. Chem.* **2012**, *3*, 2006−2010. (b) Zawaneh, P. N.; Doody, A. M.; Zelikin, A. N.; Putnam, D. *Biomacromolecules* **2006**, *7*, 3245−3251. (c) Viel, S.; Mazarin, M.; Giordanengo, R.; Phan, T. N. T.; Charles, L.; Caldarelli, S.; Bertin, D. *Anal. Chim. Acta* **2009**, *654*, 45−48.
(28) Kraka, E.; Cremer, D. *Acc. Chem. Res.* **2010**, *43*, 591−601.
(29) (a) Jeon, J. Y.; Eo, S. C.; Varghese, J. K.; Lee, B. Y. *Beilstein J. Org. Chem.* **2014**, *10*, 1787−1795. (b) Duan, Z.; Wang, X.; Gao, Q.; Zhang, L.; Liu, B.; Kim, I. *J. Polym. Sci., Part A: Polym. Chem.* **2014**, *52*, 789−795.
(30) (a) Liu, Y.; Xiao, M.; Wang, S.; Xia, L.; Hang, D.; Cui, G.; Meng, Y. *RSC Adv.* **2014**, *4*, 9503−9508. (b) Sun, X.-K.; Zhang, X.-H.; Chen, S.; Du, B.-Y.; Wang, Q.; Fan, Z.-Q.; Qi, G.-R. *Polymer* **2010**, *51*, 5719−5725. (c) Liu, Y.; Huang, K.; Peng, D.; Wu, H. *Polymer* **2006**, *47*, 8453−8461. (d) Liu, Y. L.; Deng, K. R.; Wang, S. J.; Xiao, M.; Han, D. M.; Meng, Y. Z. *Polym. Chem.* **2015**, *6*, 2076−2083.
(31) Brown, N. J.; Harris, J. E.; Yin, X.; Silverwood, I.; White, A. J. P.; Kazarian, S. G.; Hellgardt, K.; Shaffer, M. S. P.; Williams, C. K. *Organometallics* **2014**, *33*, 1112−1119.
(32) (a) Moore, D. R.; Cheng, M.; Lobkovsky, E. B.; Coates, G. W. *J. Am. Chem. Soc.* **2003**, *125*, 11911−11924. (b) Brombacher, H.; Vahrenkamp, H. *Inorg. Chem.* **2004**, *43*, 6042−6049. (c) Felix, A. M.; Boro, B. J.; Dickie, D. A.; Tang, Y. J.; Saria, J. A.; Moasser, B.; Stewart, C. A.; Frost, B. J.; Kemp, R. A. *Main Group Chem.* **2012**, *11*, 13−29. (d) Rit, A.; Spaniol, T. P.; Okuda, J. *Chem. - Asian J.* **2014**, *9*, 612−619. (e) Sokolowski, K.; Bury, W.; Tulewicz, A.; Cieslak, A. M.; Justyniak, I.; Kubicki, D.; Krajewska, E.; Milet, A.; Moszynski, R.; Lewinski, J. *Chem. - Eur. J.* **2015**, *21*, 5496−5503. (f) Sattler, W.; Parkin, G. *J. Am. Chem. Soc.* **2011**, *133*, 9708−9711.
(33) (a) Robert, C.; Ohkawara, T.; Nozaki, K. *Chem. - Eur. J.* **2014**, *20*, 4789−4795. (b) Liu, J.; Bao, Y.-Y.; Liu, Y.; Ren, W.-M.; Lu, X.-B. *Polym. Chem.* **2013**, *4*, 1439−1444.

DOI: 10.1021/jacs.5b13070
J. Am. Chem. Soc. 2016, 138, 4120−4131